Arabian Journal of Chemistry (2017) **10**, S404–S411

King Saud University

Arabian Journal of Chemistry

www.ksu.edu.sa
www.sciencedirect.com

ORIGINAL ARTICLE

Study of photocatalytic asset of the $ZnSnO_3$ synthesized by green chemistry

Ashok V. Borhade *, Yogeshwar R. Baste

Research Centre, Department of Chemistry, HPT Arts and RYK Science College, Nashik, 422005 MS, India

Received 6 April 2012; accepted 2 October 2012
Available online 11 October 2012

KEYWORDS

Photocatalyst;
Mechanochemical synthesis;
Green chemistry;
XRD;
TEM;
BET

Abstract In this paper, we report a simple one-step mechanochemical synthesis method with a green chemistry approach for a light-induced heterogeneous oxide photocatalyst, $ZnSnO_3$. The catalyst was characterized by various investigative techniques, like Infrared Fourier Transform Spectroscopy, Diffused Reflectance UV–visible Spectroscopy, X-ray Diffraction, Scanning Electron Microscopy, Tunnelling Electron Microscopy, and Thermogravimetric analysis to carry out structural and spectroscopic properties of the photocatalyst. The synthesized $ZnSnO_3$ particles had an average size of 105 nm with a band gap of 3.34 eV. The photocatalyst was thermally stable over a wide range of temperatures. The sunlight mediated degradation of Methyl blue, Indigo carmine and Acid violet dyes were achieved by using $ZnSnO_3$.

1. Introduction

With growing industrialization and population, environmental contamination caused by organic pollutants is being one of the overwhelming problems all over the world. However, its horrible adverse effects have appeared in the shape of environmental collapse. The domestic use and industrial activity both produce a large amount of wastewater, which then disposed into natural channels leading to a high pollution risk. A small quantity of polluted water is sufficient to contaminate much greater capacity of clean water. Synthetic dyes are toxic refractory chemicals, which generate murky colour to the water and are hazardous to the environment. The dyes were detected in a dissolved state in wastewater (Esther et al., 2004). Most of these dyes are toxic and carcinogenic in nature (Blake et al., 1999). One must note down that, a wide spectrum of compound can transform themselves into potentially dangerous substances during the water treatment process. A non-biodegradable pollutant present in wastewater is a point of major serious pain to the researchers in the world.

Various methods have been suggested for the purification of polluted water, these includes; surface adsorption (Meshko et al., 2001 and Iqbal et al., 2011), and bio-degradation (Elias et al., 2000; Saratale et al., 2009, and Shah et al., 2012), use of membrane (Joong et al., 2008). The light induced photocatalytic process has received considerable attention in the last few decades. The photocatalytic reactions on semiconductors have been utilized for many applications, such as air cleaners (Hoffmann et al., 1995), self-cleaning materials (Libby, 1971), and antibacterial materials (Wang et al., 2010).

* Corresponding author. Fax: +91 (0253) 2573097.
E-mail address: ashokborhade2007@yahoo.co.in (A.V. Borhade).

Peer review under responsibility of King Saud University.

ELSEVIER Production and hosting by Elsevier

http://dx.doi.org/10.1016/j.arabjc.2012.10.001

In photocatalysis, light used to activate a substance that alters the rate of a chemical reaction without involvement of itself. The great significance of photocatalysis process is that, it can degrade and/or detoxify various complex organic chemicals, which has not tackled by other methods of purification. Furthermore, it increases the chance of reuse of water. Generally, the reaction recognized as phenomena originating from electrons and holes excited by absorption of photons with energy greater than the band gap energy of the semiconductors. The holes have a strong potential to draw electrons out of organic and inorganic contaminants, resulting in the decomposition of hazardous materials, such as dyes, (Borhade and Baste, 2011 and Lodha et al., 2011), pesticides (Lafi and Al-Qodah, 2006), fungicides (Fenoll et al., 2011) and insecticides (Kitsiou and Filippidis, 2009), and many organic pollutants. When aqueous suspension of the photocatalyst was irradiated with light energy greater than the band gap energy of the semiconductor oxide, conduction band electrons (e^-) and valance band holes (h^+) are formed. The photogenerated electrons react with absorbed molecular O_2 reducing it to superoxide radical anion $O_2^{\cdot}$, and photogenerated holes can oxidize organic molecules directly or the OH and the H_2O molecule adsorbed at catalyst surface to OH radical. These electron hole pairs act as a strong oxidizing agent and can easily attack on organic molecules or those located close to the surface of the catalyst, thus leading to complete degradation of organic molecules.

Literature survey shows that, very little attention is given to the mixed oxide photocatalyst. The TiO_2 is widely studied and demonstrated its photocatalytic activity (Chen and Weiwei, 2009; Konstantinou and Albanis, 2004; Gupta et al., 2011). The ZnO is another broadly studied photocatalyst for the dye degradation (Chakrabarti and Dutta, 2004; Daneshvar and Salari, 2008). Few reports are available on the studies related to the photocatalytic activity of coupled semiconductor photocatalyst, such as TiO_2–CeO_2 (Baoshun and Xiujian, 2005), TiO_2–WO_3 (Bojinova et al., 2008), TiO_2–SnO_2 (Tada et al., 2000) and ZnO–SnO_2 (Wang et al., 2004; Azam and Ali, 2011).

As far as degradation of Methyl blue, Indigo carmine and Acid violet is concerned, different researchers have worked and efficiently degraded the dyes. Madhu et al. (2009) degraded Methyl blue in 120 min with TiO_2 and in presence of H_2O_2 at different concentrations. Tianyong Zhang et al. and Kuo degraded Methyl blue with TiO_2 by adjusting pH of the solution (Tianyong et al., 2001; Kuo and Ho, 2001), and N. Barka degraded Indigo carmine by TiO_2-coated non-woven fibre by adjusting pH and temperature (Barka et al., 2008). Krushnakumar and Swaminathan (2012) have degraded Acid violet-7 using direct sunlight at pH-12. The study follows pseudo first order kinetics but, all above study is not environmentally friendly. The main advantage of photocatalytic is that, the process takes place at ambient temperature without overpressure. The oxygen used for oxidation can be directly obtained from atmosphere.

We report the synthesis of $ZnSnO_3$ photocatalyst by simple one-pot mechanochemical method using a green chemistry approach. Various routine methods are available for the synthesis of mixed metal oxide such as; sol–gel (Gao et al., 2002; Wongkalasin et al., 2011), hydrothermal (Bao et al., 2005; Lee et al., 2012) and thin film vapour deposition method (Sun and Wang, 2008). These methods are complicated, cost effective and cause environmental pollution. Whereas the solid-state mechanochemical synthesis method is an environmentally friendly method, easy, and also gives less energy to the environment (Yoon and Ischay, 2010). The structural properties of the synthesized $ZnSnO_3$ photocatalyst were approved by various techniques like, FTIR, UV-DRS, XRD, SEM, TEM, BET surface area and TGA. The aim of the present work was to investigate the degradation of Methyl blue (MB; colour index-42780), Indigo carmine (IC; colour index-75781) and Acid violet (AV; colour index-60730) in aqueous $ZnSnO_3$ suspension under sunlight irradiation.

2. Experimental

2.1. Synthesis of $ZnSnO_3$ photocatalyst

Apart from reported methods we have synthesized mixed metal oxide photocatalyst using a green chemistry approach. Starting reagents were of ZnO (Merck, Batch No. MD6M561095 CAS No 1314-13-2, 99.9% pure) and SnO_2 (Loba Chem. Batch No. 27685, CAS No 18282-10-5, 99.9% pure). Equimolar mixture of ZnO and SnO_2 was grinded with mortar and pestle to acquire fine powder for 20 min and calcinated at 500 °C for 3 h. Again the obtained powder was further calcinated at 800 °C following milling after each interval of three-hour time. The calcination was continued for next twenty hours with milling. Afterwards, at the end mixture was heated up to the terminal temperature. The furnace was programmed as 10 °C per min from one temperature to subsequent higher temperatures. The product $ZnSnO_3$, thus obtained, was used for characterization.

2.2. Characterization

The vibrational frequency in the range of 400–4000 $cm^{-1}$of the synthesized catalyst was studied by FTIR, 8400S-Shimadzu. The optical property of $ZnSnO_3$ photocatalyst was evaluated by scanning over the wavelength range of 200–800 nm by using Perkin Elmer-λ-950, UV–visible spectrophotometer. The structural properties of the material were studied by using X-ray diffractometer, Rigaku-D/MAX-2500 with Cu-Kα radiation, with $\lambda = 1.5406$ Å. The surface morphology and chemical compositions of the synthesized catalyst were analysed by using a scanning electron microscope JEOL, JED-2300LA, coupled with an energy dispersive spectrometer-JED-2300LA. The TEM images were recorded on Philips, CM-200. The Surface area (S_{BET}), pore volume(V_p) and pore diameter (D_p) were evaluated by Quntachrome Autosorb automated gas sorption system, Autosorb-1 NOVA-1200 and Mercury Porositymeter Autosoeb-IC. The stability of the catalyst was evaluated by thermogravimetric analysis on Perkin Elmer-TG, Thermogravimetric analyzer.

2.3. Photocatalytic activity

The photocatalytic activity of the synthesized $ZnSnO_3$ photocatalyst was evaluated by studying degradation of Methyl blue, Indigo carmine, and Acid violet dyes. Experiments were conducted with 20 and 10 ppm dye solution: with 6 and 10 g/L photocatalyst to study the effect of amount of dye concentration and amount of catalyst concentration on degradation.

During the experiment, three types of observations were recorded. In one set of the experiment, dye solution (20 and 10 ppm) was irradiated with the $ZnSnO_3$ photocatalyst, 6 g/L (0.3 g catalyst in 50 ml) and 10 g/L (0.5 g catalyst in 50 ml) in the presence of sunlight. A similar second set was kept in the dark. The third set containing only dye solution was exposed to sunlight. The decrease in the absorbance due to the photodegradation of dyes was measured on systronics double beam spectrophotometer after every 30 min. The sunlight intensity was monitored by using Lux meter Kusam-meko, KMLUX.

3. Results and discussion

3.1. Characterization of $ZnSnO_3$

The infrared absorption spectra of SnO_2, ZnO (starting material) and $ZnSnO_3$, (photocatalyst) are shown in Fig. 1. (a–c), The IR spectra show, the vibrational frequency at 425 cm^{-1} indicates the presence of Zn–O and frequency band at around 600 cm^{-1} indicates the presence of Sn–O vibrations in SnO_2 and $ZnSnO_3$.

In Fig. 2, (a) represents X-ray powder diffraction pattern for SnO_2. The d-line pattern of the X-ray diffraction pattern matches with the standard JCPDS data card No. 21-1250. The peaks at scattering angles at 26.64, 33.98, 38.06, 51.81, 57.87, 61.95, 64.87, 66.26, and 71.39 correspond to the 110, 101, 200, 211, 002, 310, 112, 301, and 202 crystal planes (*hkl*) respectively showing tetragonal structure of SnO_2. Fig. 2b shows X-ray powder diffractogram of the pure ZnO powder. The d-line pattern of the X-ray diffractogram matches with the standard JCPDS data card No. 79-0206. The peaks at scattering angles at 31.76, 34.44, 36.31, 47.73, 56.71, 63, 68.01, and 69.18 correspond to the plane 100, 002, 101, 102, 110, 103, 112, and 201 crystal planes (*hkl*) respectively showing hexagonal type structure. Fig. 2c shows X-ray powder profile of the synthesized $ZnSnO_3$ powder. The d-line pattern of the X-ray diffractogram matches with the standard JCPDS data card No. 28-1486. These peaks at scattering angles at of 29.13, 34.3, 35.84, 51.8 and 60.4 correspond to the reflection from 220, 311, 222, 422, and 440 crystal planes (*hkl*) respectively and thus confirming the orthorhombic structure of the $ZnSnO_3$.

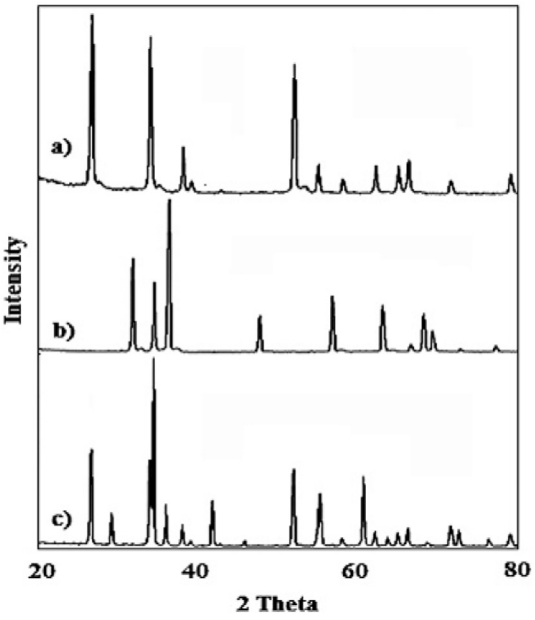

Figure 2 XRD pattern of (a) SnO_2, (b) ZnO, and (c) $ZnSnO_3$.

Fig. 3 represents the UV–visible diffused reflectance spectra of (a) SnO_2, (b) ZnO and (c) synthesized $ZnSnO_3$ photocatalyst. The UV–visible diffused reflectance spectrum of SnO_2 shows absorption edge cuts in the region of 344 nm giving a band gap ($E_g = hc/\lambda$) value of 3.6 eV, ZnO absorption edge cuts at 369 nm showing a band gap of 3.36 eV. The diffused reflectance spectrum depicts that the absorption goes into UV–visible region. The UV-DRS of the $ZnSnO_3$ has absorption edge cut-off at 370 nm with a corresponding band in the

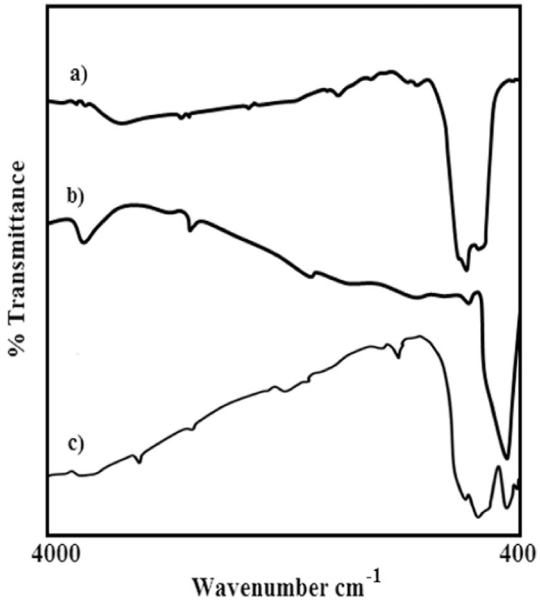

Figure 1 IR spectra of (a) SnO_2, (b) ZnO, and (c) $ZnSnO_3$.

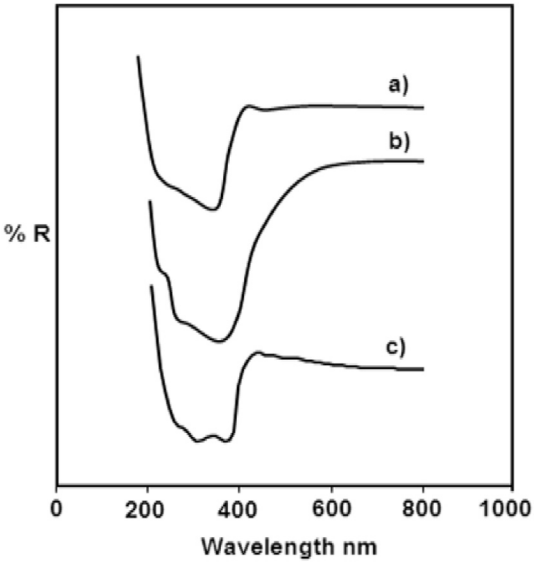

Figure 3 UV–visible DRS spectra of (a) SnO_2, (b) ZnO, and (c) $ZnSnO_3$.

visible region. The band gap energy for the synthesized compound was found to be 3.37 eV. The result implies that the $ZnSnO_3$ catalyst may possess excellent photocatalytic activity.

The surface morphology and associated chemical composition of synthesized photocatalyst were achieved by using a scanning electron microscope (SEM) coupled with EDAX. It is clear from the Fig. 4 that, very fine particles of $ZnSnO_3$ are joined to each other forming the cluster of particles. It appears from the SEM micrograph indicates the polycrystalline nature of $ZnSnO_3$. The EDAX data furnish elemental composition in conformity with the respective molar proportions taken. The observed mass percentage of Zn is 21.41%, Sn in the $ZnSnO_3$ is 58.49% and that of oxygen is 20.10%, which confirm the formation of $ZnSnO_3$.

The TEM image along with the selected area of the diffraction pattern (SAED) recorded for the sample corresponding to the $ZnSnO_3$ is shown in Fig. 5. The dark spot in the SEAD micrograph can be alluded to $ZnSnO_3$ nanoparticles. The SAED pattern associated with such spot reveals occurrence of $ZnSnO_3$ is in good agreement with XRD data. The planes 311 and 440 are shown in SAED image. It is clear from the TEM image that, the average particle size of the $ZnSnO_3$ crystallites is 105 nm.

Fig. 6 shows Nitrogen adsorption–desorption isotherm and the pore size distribution plots calculated from the desorption branch of N_2 isotherm by the Barret, Joyner and Halenda (BJS) method of the $ZnSnO_3$ material. The pore size distribution showed a narrow range for synthesized photocatalyst, $ZnSnO_3$, implying good homogeneity of the pore. The surface area (S_{BET}); is 28.30 m^2/g, pore volume (V_p); is 0.0299 cc/g, and pore diameter (D_p); is 24.48 Å for the synthesized material.

The thermal stability of the photocatalyst was performed by thermogravimetric analysis Fig. 7. It is observed that, no significant loss in mass on rise in temperature was observed when the material was heated up to 700 °C. The photocatalyst was found to be very stable over a wide range of temperatures.

3.2. Photocatalytic property of $ZnSnO_3$

Photocatalytic activity evaluations of $ZnSnO_3$ were performed by photodegradation of Methyl blue, Indigo carmine, and Acid violet dyes in an aqueous solution (10 and 20 ppm) under

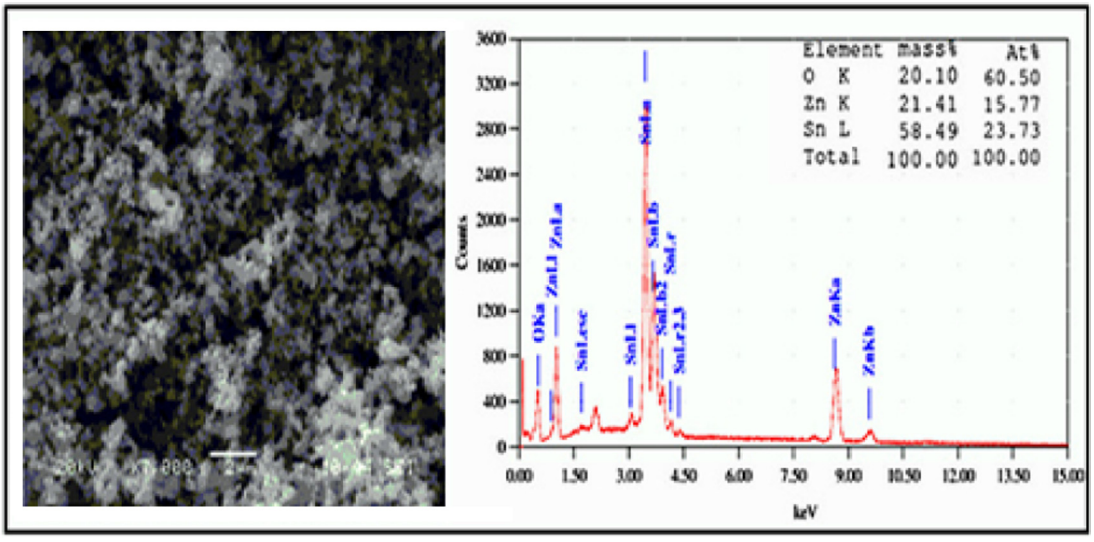

Figure 4 SEM and EDAX of $ZnSnO_3$ photocatalyst.

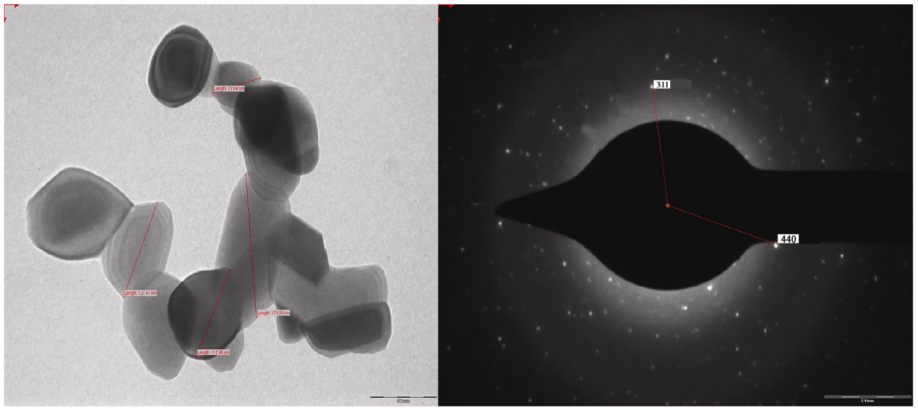

Figure 5 TEM and SEAD images of the $ZnSnO_3$.

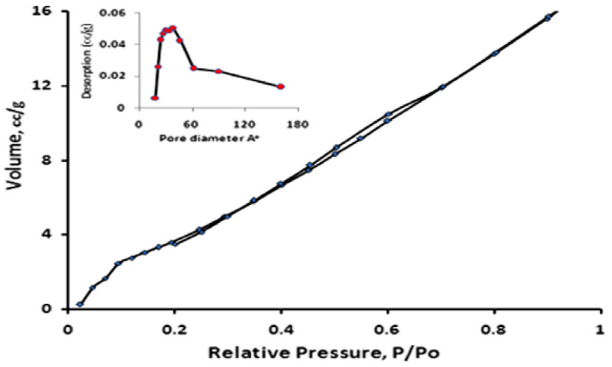

Figure 6 BET surface area, pore volume and pore size of the photocatalyst $ZnSnO_3$.

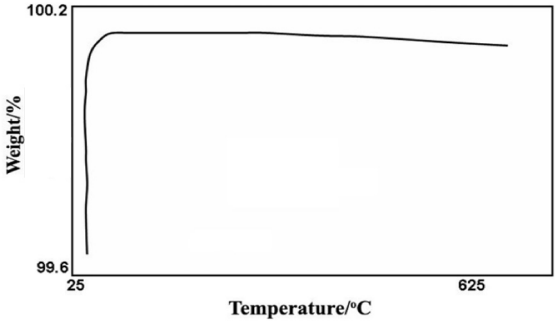

Figure 7 Thermogram of $ZnSnO_3$.

simulated sunlight. The photodegradation of the dyes was studied by measuring the decrease in the absorbance after every 30 min on the double beam spectrophotometer. The irradiation intensity is variable from one day to other and from one hour to other in the same day. The sunlight intensity was monitor by Lux meter. The lowest and highest sunlight intensity during the experiment was 0.01098 and 0.0139 W/cm^2 respectively and is indicated in Fig. 8.

Fig. 9 depicts the graphical representation of percentage degradation of the dyes with time for $ZnSnO_3$ catalyst 6 g/L (0.3 g catalyst in 50 ml dye solution). In the decolourization-time profiles, the series-p1, p2 and p3 indicate degradation of methyl blue, series q1, q2 and q3 indicate degradation of indi-

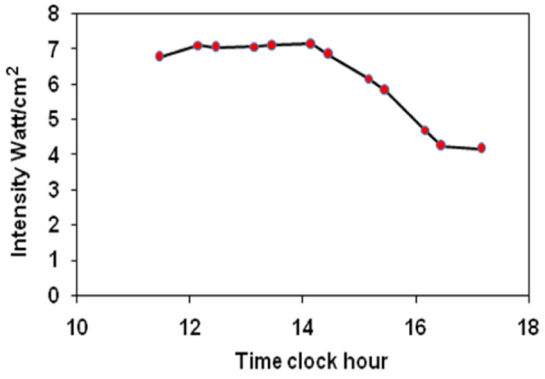

Figure 8 Variation of light intensity measurement using LUX meter.

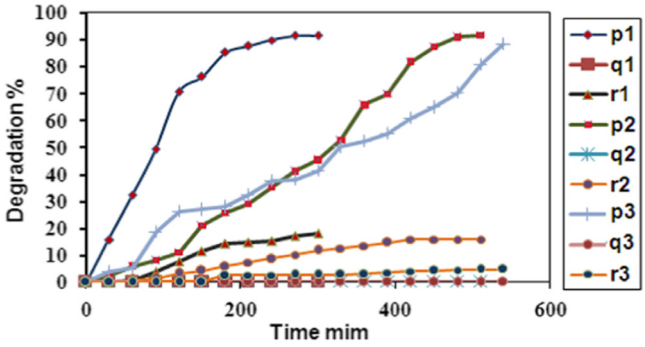

Figure 9 Degradation of dye (6 g/L photocatalyst, 20 ppm dye solution).

go carmine, and series-r1, r2 and r3 indicate degradation of acid violet. In the figure, the curves p1, q1, and r1 represent the rapid degradation of the dye solution in the presence of the $ZnSnO_3$ photocatalyst (6 g/L) when irradiated with sunlight. The curves p_2, q_2, and r_2 of the graph indicate no decrease in the absorbance when the dye solution was kept in the dark in the presence of the photocatalyst. It reveals that, no photochemical reactions were going on in the absence of the light and in the presence of the catalyst. The curves p_3, q_3, and r_3 indicate that there was no measurable change in the absorbance when dye solutions were kept in the light and in the absence of the photocatalyst. This proves that, the degradation occurs only in the presence of the photocatalyst, $ZnSnO_3$ and in the presence of sunlight.

Fig. 10 represents degradation of dyes when 10 g/L (0.5 g catalyst in 50 mL) catalyst was employed to 20 ppm of dye solution. In the figure, p4, p5, and p6 indicate degradation of methyl blue; curves q4, q5 and q6 indicate degradation of Indigo carmine dye; curves r4, r5, and r6 indicate degradation of Acid violet dye. Further, curve p4, q4 and r4 reveals that on increased amount of photocatalyst (10 g/L) enhances the degradation of MB, IC, and AV dyes..

Fig. 11 explains the study, when 6 g/L (0.3 g catalyst in 50 ml) with 10 ppm dye solution was used for degradation. In the figure curves ×1, ×2, and ×3 indicate degradation of Methyl blue, curves y1, y2, and y3 indicate degradation of Indigo carmine, and curves z1, z2, and z3 indicate degradation of Acid violet dye. Whereas curves x1, y1, and z1 represent faster degradation when dye solution containing photocatalyst was irradiated to sunlight.

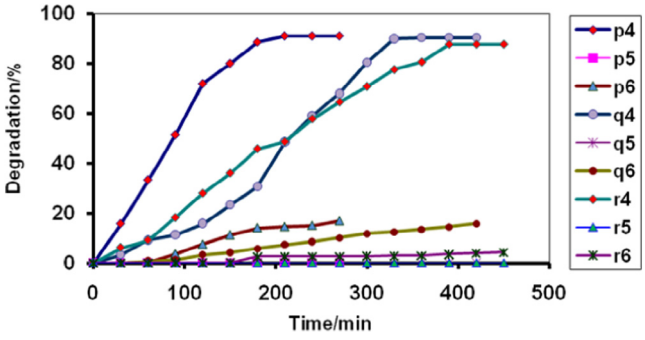

Figure 10 Degradation of dye (10 g/L photocatalyst, 20 ppm dye solution).

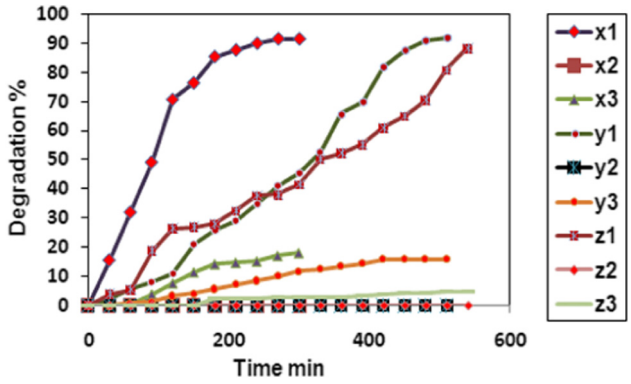

Figure 11 Degradation of dye (6 g/L photocatalyst, 10 ppm dye solution).

Fig. 12 explains the study, when 10 g/L (0.5 g catalyst in 50 ml) with 10 ppm dye solution was used for degradation. In the same figure, degradation of Methyl blue is indicated by curves ×4, ×5, and ×6, degradation of Indigo carmine is indicated by curves y4, y5, and y6 and degradation of Acid violet is indicated by curves z4, z5, and z6. It is observed that, x4, y5, and z6 represent faster degradation when dye solution containing photocatalyst was irradiated to sunlight. In both the cases, the effect of amount of catalyst yields faster degradation. This may be due to an increase in amount of the photocatalyst, which increases ejection of number of electrons-hole pair in the conduction band and in the valence band respectively.

Fig. 13 shows the degradation of dyes before and after exposure to sunlight and photocatalyst. In Fig. 13, X, Y, and Z represent UV–visible absorption spectrum of MB, IC, and AV dyes, respectively before exposure to sunlight and photocatalyst and X1, Y1, and Z1 indicate UV–visible absorption spectrum of MB, IC, and AV dyes respectively due to degradation. It is found that, before exposed to sunlight and photocatalyst the chromophoric absorption peaks of MB, IC, and AC dyes were at 670, 610, and 685 nm respectively. After exposed to sunlight and $ZnSnO_3$ photocatalyst, peaks were eventually disappeared, and new peaks at 190, 217, and 245 nm appeared due to the degradation of MB, IC, and AC dyes respectively.

The reaction rate for photocatalytic reactions is given as follows.

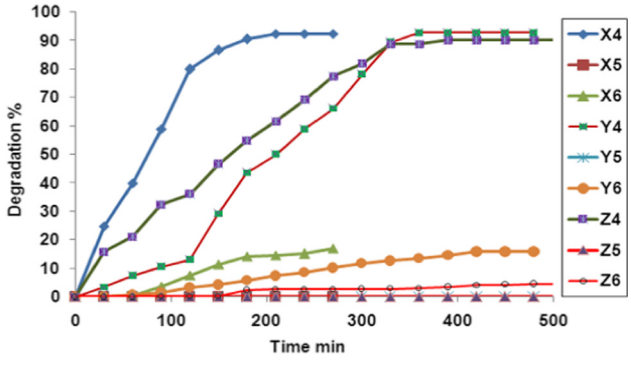

Figure 12 Degradation of dye (10 g/L photocatalyst, 10 ppm dye solution).

$$\frac{-dC_{dye}}{dt} = k \times C_{dye} \times C_{OH\cdot} \quad (1)$$

Where C_{dye} represents the dye concentration in ppm; $C_{OH\cdot}$ represents hydroxyl concentration in ppm. The reaction rate for photocatalytic reactions is independent of hydroxyl concentration. The $C_{OH\cdot}$ can be considered to be constant. The rate Eq. (1) can be simplified to

$$\frac{-dC_{dye}}{dt} = k \times C_{dye} \quad (2)$$

Integrating above equation from C_{dye0} to C_{dye} on the left hand side and 0 to t to the right

$$\int_{C_{dye0}}^{C_{dye}} -dC_{dye} = k \int_0^t dt$$

$$\ln\left(\frac{C_{dye0}}{C_{dye}}\right) = kt \quad (3)$$

where C_{dye0} represents initial dye concentration in ppm and k is pseudo first order rate constant, t is time in min. C_{dye} represents final dye concentration.

The degradation process follows pseudo first order kinetics and is shown in Fig. 14. The rate constants obtained are 0.01178, 0.003372, and 0.002739 min^{-1} for MB, IC, and AV dyes respectively. Photocatalysis is a destructive technology leading to complete degradation of organic molecules. The probable mechanism involved for the degradation of studied dyes can be explained as follows.

Absorption of an efficient photon ($hv \geqslant E_g = 3.37$ eV) by zinc stannate

$$(ZnSnO_3) + hv \rightarrow e^-_{CB} + h^+_{VB}; \quad (1)$$

Oxygen ion absorption

$$(O_2)_{ads} + e^-_{CB} \rightarrow O_2^{\cdot-} \quad (2)$$

Neutralization of OH^- groups into $OH^{\cdot}$ radical by photoholes

$$(H_2O \leftrightarrow H^+ + OH^-)_{ads} + h^+_{VB} \rightarrow H^+ + OH^{\cdot} \quad (3)$$

Oxidation of organic dyes (Methyl blue, Indigo carmine and Acid violet) via successive attacks by $OH^{\cdot}$ radicals,

$$R + h^+ \rightarrow {}^{\cdot}R + H_2O \quad (4)$$

or by direct reaction with holes

$$R + h^+ \rightarrow R^+ \rightarrow \text{degraded product} \quad (5)$$

Considering the last process, holes react directly with carboxylic acid, generating CO_2 by way of the photo-Kolbe (Bernhard et al., 1978) reaction.

$${}^{\cdot}R + O_2 \rightarrow ROO^{\cdot} + \rightarrow CO_2 \quad (6)$$

On the basis of experimental, a tentative mechanism for photocatalytic degradation of dye may be proposed as, the photocatalyst $ZnSnO_3$, absorbs radiations of suitable wavelength electrons from valence bond are promoted to the conduction band to produce an electron hole pair. These entities migrate to the catalyst surface; the electron vacancy reacts easily with surface bound H_2O to produce $OH^{\cdot}$ radicals, whereas electrons react with O_2 to produce superoxide radical anion of oxygen, $O_2^{\cdot-}$. The $OH^{\cdot}$ and $O_2^{\cdot-}$ produced in an above manner then react with dye (MB, IC and AV) to form other species leading to the colourless product; i.e., degradation of the dye. The probable

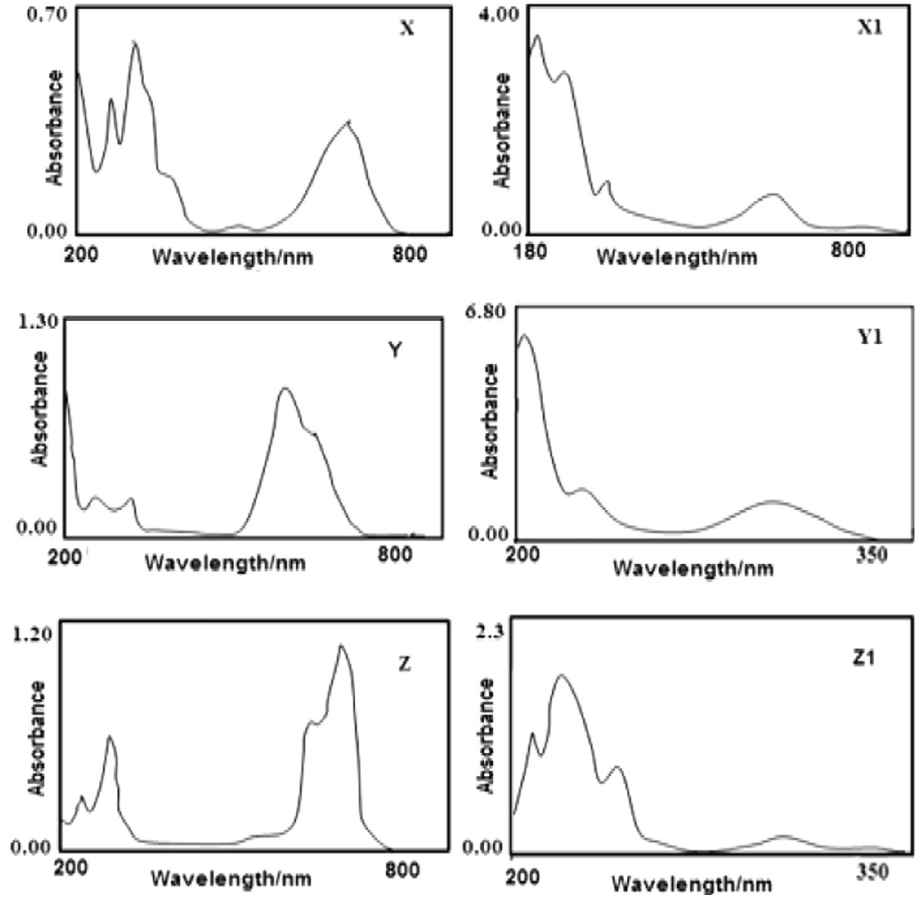

Figure 13 UV–visible spectra of dyes before and after exposure to sunlight.

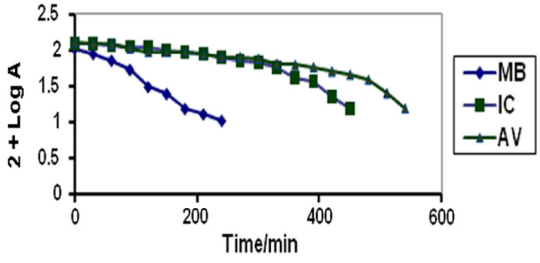

Figure 14 Kinetic study of degradation of MB, IC and AV dyes.

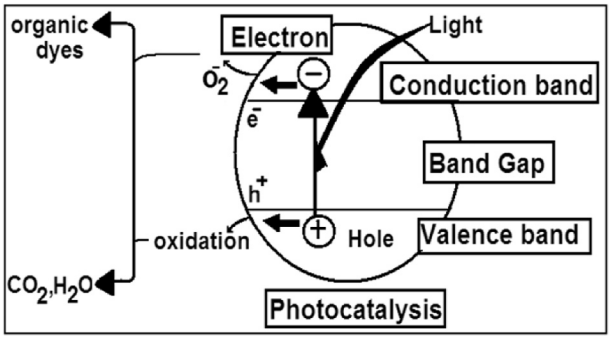

Figure 15 General pathway of dye degradation.

mechanism of degradation of MB, IC and AV dyes is schematically shown in Fig. 15.

4. Conclusions

The polycrystalline novel photocatalyst, $ZnSnO_3$ was synthesized by green chemistry using a solid state mechanochemical method followed by calcinations. Its mean size, band gap energies as well as its photocatalytic activities are studied in detail. $ZnSnO_3$ photocatalysis is capable of mineralizing the dyes without affecting aquatic life. The decay followed pseudo first order kinetic to the visible absorption of the test dyes. The effective photodegradation of dyes by $ZnSnO_3$ photocatalyst under stimulated sunlight is a very exciting aspect in the photocatalytic area, and this work may provide new insight into the development of novel sunlight photocatalyst. Degradation was found to be the highest with 10 ppm solution of MB, IC and AV dyes with 10 g/L of $ZnSnO_3$ photocatalyst.

Acknowledgements

Authors are thankful to the University Grant Commission, New Delhi, University of Pune for financial support to carry out this work and Dr. A.V. Mahajan, Department of Physics, Indian Institute of Technology, Powai, Mumbai for X-ray analysis.

References

Azam, A.F., Ali, R.M., 2011. World Acad. Sci. Eng. Technol. 76, 138–140.

Bao, X., Yan, S., et al., 2005. Mater. Lett. 59 (4), 412–415.

Baoshun, L., Xiujian, Z., 2005. Surf. Sci. 595, 203–211.

Barka, N., Assabbane, A., et al., 2008. J. Hazard. Mater. 152, 1054–1059.

Bernhard, K., Clarine, D., Allen, J., 1978. J. Am. Chem. Soc. 100 (15), 4903–4905.

Blake, D., Maness, P., et al., 1999. Sep. Purif. Methods 28 (1), 1–50.

Bojinova, AS., Papazova, CI., Eu, J., 2008. Anal. Chem. 3, 34–43.

Borhade, A.V., Baste, Y.R., 2011. J. Therm. Anal. Cal., 1–7.

Chakrabarti, S., Dutta, B.K., 2004. J. Hazard. Mater. 112 (3), 269–278.

Chen, F., Weiwei, Z., 2009. Catal. Commun. 10, 1510–1513.

Daneshvar, N., Salari, D., 2008. J. Hazard Mater. 156, 194–200.

Elias, A., Silgia, C., et al., 2000. Appl. Environ. Microbiol., 3357–3362.

Esther, F., Tibor, C., Gyula, O., 2004. Environ. Int. 30, 953–971.

Fenoll, J., Ruiz, E., et al., 2011. Chemosphere 85 (8), 1262–1268.

Gao, Y., Yu, W., et al., 2002. Chin. Chem. Lett. 13 (11), 1115–1118.

Gupta, VK., Jain, R., et al., 2011. Mater. Sci. Eng. 31 (5), 1062–1067.

Hoffmann, M.R., Martin, S.T., et al., 1995. Chem. Rev. 95, 69–96.

Iqbal, J., Watto, H., et al., 2011. Arab. J. Chem. 4, 389–395.

Joong, H., Yong, H., et al., 2008. Dyes Pigm. 76, 429–434.

Kitsiou, V., Filippidis, N., 2009. Appl. Catal. B 86, 27–35.

Konstantinou, L., Albanis, T., 2004. Appl. Catal. B Environ. 49 (1), 1–14.

Krushnakumar, B., Swaminathan, M., 2012. Ind. J. Chem. 51A, 580–585.

Kuo, W.S., Ho, P.H., 2001. Chemosphere 45, 77–73.

Lafi, W., Al-Qodah, Z., 2006. J. Hazard. Mater. 137, 489–497.

Lee, W.W., Huang, S.T., et al., 2012. J. Mol. Catal. A: Chem. 361–362, 80–90.

Libby, W.F., 1971. Science 171 (3970), 499–500.

Lodha, S., Jain, A., Punjabi, P., 2011. Arab. J. Chem. 4, 383–387.

Madhu, G.M. et al., 2009. J. Environ. Biol. 30 (2), 259–264.

Meshko, V., Markovska, L., et al., 2001. Water Res. 35 (14), 3357–3366.

Saratale, R.G., Saratale, G.D., et al., 2009. J. Hazard. Mater. 166, 1421–1428.

Shah, P.D., Dave, S.R., Rao, M.S., 2012. Int. Biodeterior. Biodegradation 69, 41–50.

Sun, H., Wang, C., 2008. J. Non-Cryst. Solids 354 (12–13), 1440–1443.

Tada, H., Hattori, A., et al., 2000. J. Phys. Chem. B 104 (19), 4585–4587.

Tianyong, Z., et al., 2001. J. Photochem. Photobiol. Chem. A 140, 163–172.

Wang, C., Wang, X., et al., 2004. J. Photochem. Photobiol., A 168, 47–52.

Wang, H., Yang, H., et al., 2010. Chin. J. Process Eng. 10 (5), 1025–1029.

Wongkalasin, P., Chavadej, S., Sreethawong, T., 2011. Colloids Surf., A 384 (1-3), 519–528.

Yoon, T., Ischay, M., 2010. Nat. Chem. 2, 527–532.